EARTHQUAKE ENGINEERING AND STRUCTURAL DYNAMICS, VOL. 25, 1211–1230 (1996)

OPTIMAL POLYNOMIAL CONTROL FOR SEISMICALLY EXCITED NON-LINEAR AND HYSTERETIC STRUCTURES

J. N. YANG*, A. K. AGRAWAL† AND S. CHEN‡

Department of Civil and Environmental Engineering, University of California, Irvine, CA 92715, U.S.A.

SUMMARY

In this paper, we present an optimal polynomial controller for reducing the peak response quantities of seismically excited non-linear or hysteretic building systems. A performance index, that is quadratic in control and polynomial of any order in non-linear states, is considered. The performance index is minimized based on the Hamilton–Jacobi–Bellman equation using a polynomial function of non-linear states, which satisfies all the properties of a Lyapunov function. The resulting optimal controller is a summation of polynomials in non-linear states, i.e. linear, cubic, quintic, etc. Gain matrices for different parts of the controller are determined from Riccati and Lyapunov matrix equations. Numerical simulation results indicate that the percentage of reduction for the selected peak response quantity increases with the increase of the earthquake intensity. Such load adaptive properties are very desirable, since the intensity of the earthquake ground acceleration is stochastic in nature. The proposed optimal polynomial controller is an effective and viable control method for non-linear or hysteretic civil engineering structures. It is an addition to available control methods in the literature.

KEY WORDS: optimal structural control; polynomial control; non-linear control; seismic response; non-linear structures; hysteretic structures; structural dynamics

INTRODUCTION

Aseismic hybrid protective systems, consisting of a combination of active control devices and passive base isolation systems, have been shown to be quite effective. Since the dynamic behaviour of most base isolation systems, such as lead-core rubber bearings or frictional-type sliding bearings, is highly non-linear or inelastic, hybrid protective systems involve control of non-linear or hysteretic structural systems. Likewise, under strong earthquakes, yielding may occur even if the fixed-base building is equipped with active control systems. As a result, control of non-linear or hysteretic civil engineering structures has attracted considerable attraction recently. Various control methods have been investigated, including pulse control,[1] polynomial control,[2] acceleration control,[3–5] instantaneous optimal control,[6] dynamic linearization,[7,4] non-linear control,[8–10] neural network,[11] sliding mode control,[12–19] etc.

Under strong earthquakes, the main objective of active/hybrid control is to reduce the peak (maximum) response quantities of the structure, such as peak interstorey drifts, in order to minimize the damage. Unfortunately, it is very difficult to obtain a controller that minimizes the peak response quantities of either linear or non-linear structures. As a result, it has been advocated in a keynote paper[20] at The First World Conference on Structural Control that non-linear controllers, such as polynomial controllers, should be studied for civil engineering applications, even for linear structures. For linear structures, it has been shown by Wu *et al.*,[21] Tomasula *et al.*[22] and Agrawal and Yang[23,24] that the polynomial controller is more effective than the classical linear controller in suppressing the peak response, because of its ability to apply bigger

*Professor
†Graduate Assistant
‡Visiting Associate Researcher

CCC 0098–8847/96/111211–20

Received 31 August 1995
Revised 10 May 1996

control force under strong earthquakes. For non-linear or hysteretic structures, it has been shown by Yang *et al.*[8,9] that a controller, having the same non-linear characteristics as that of the structure, performs better than a linear controller. In fact, the sliding mode controller also has such characteristics.[12,13]

In this paper, we present an optimal polynomial controller for the peak response reduction of seismically excited non-linear or hysteretic structures. The performance index to be minimized is quadratic in control and polynomial of any order in non-linear states. Based on the Hamilton–Jacobi–Bellman equation and the optimality conditions derived by Bernstein[25] for the non-linear optimal control problem, the performance index is minimized. The resulting optimal control law is a summation of polynomials of different orders in non-linear states, i.e. linear, cubic, quintic, etc. Gain matrices for different parts of the controller are computed easily from Riccati and Lyapunov matrix equations.

Numerical simulations have been conducted for control of a base-isolated building using lead-core rubber bearings and a fixed-base yielded building to investigate the performance of the optimal polynomial controller with respect to various control objectives, including the peak response reductions, peak control force and required control effort. The advantages of the proposed optimal polynomial controller are demonstrated by numerical simulation results.

PROBLEM FORMULATION

Consider an n-degree-of-freedom non-linear building structure subjected to a one-dimensional earthquake ground acceleration $\ddot{x}_0(t)$. The vector equation of motion is given by

$$M\ddot{X}(t) + F_c[\dot{X}(t)] + F_s[X(t)] = HU(t) + \eta\ddot{x}_0(t) \tag{1}$$

in which $X(t) = [x_1, x_2, \ldots, x_n]^T$ is an n-vector with $x_i(t)$ being the drift of a designated ith storey unit; $U(t) = [u_1, u_2, \ldots, u_r(t)]^T$ is an r-vector consisting of r control forces; superscript T denotes the transpose of a vector or a matrix; and η is an n-vector denoting the influence of the earthquake excitation. In equation (1), M is an $(n \times n)$ mass matrix; H is an $(n \times r)$ matrix denoting the location of r controllers; $F_c[\dot{X}(t)] = F_c$ is an n-vector denoting the non-linear damping force; and $F_s[X(t)] = F_s$ is an n-vector denoting the non-linear stiffness which is assumed to be a function of $X(t)$. In the state space, equation (1) becomes

$$\dot{Z}(t) = q(Z(t)) + BU(t) + E(t) \tag{2}$$

where $Z(t) = [X^T(t), \dot{X}^T(t)]^T$ is a $2n$ state vector; $q(Z(t))$ is a $2n$ non-linear vector; B is a $(2n \times r)$ location matrix for controllers; and $E(t)$ is a $2n$ excitation vector, respectively, given by

$$q(Z(t)) = \begin{bmatrix} \dot{X}(t) \\ -M^{-1}[F_c + F_s] \end{bmatrix}; \quad B = \begin{bmatrix} 0 \\ M^{-1}H \end{bmatrix}; \quad E(t) = \begin{bmatrix} 0 \\ M^{-1}\eta\ddot{x}_0(t) \end{bmatrix} \tag{3}$$

The minimization of a general non-linear performance index, subject to the constraint of the state equation in equation (2), is not amenable to analytical solutions. In the present study, we present the minimization of a polynomial performance index for the infinite time regulator problem given by

$$J = \int_0^\infty \left[q^T Q q + \ddot{X}_a^T Q_a \ddot{X}_a + U^T R U + \sum_{i=2}^{k} (q^T M_i q)^{i-1} q^T Q_i q + \bar{h}(q) \right] dt \tag{4}$$

where the implicit dependence of $U(t)$ and $q(Z(t))$ on t has been dropped and $q = q(Z)$ has been used for simplicity. In equation (4), Q is a $(2n \times 2n)$ positive semi-definite weighting matrix for non-linear states q of the system; $\ddot{X}_a = \ddot{X}_a(t)$ is an n-vector consisting of absolute accelerations for all floors; Q_a is a positive semi-definite weighting matrix; R is a $(r \times r)$ positive-definite control weighting matrix; Q_i, $i = 2, 3, \ldots, k$, are $(2n \times 2n)$ positive semi-definite weighting matrices, M_i, $i = 2, 3, \ldots, k$, are $(2n \times 2n)$ appropriate positive-definite matrices to be defined later; and $\bar{h}(q)$ is given by

$$\bar{h}(q) = \bar{h}_1(q) = \left[\sum_{i=2}^{k} (q^T M_i q)^{i-1} q^T M_i \Lambda \right] B \bar{R}^{-1} B^T \left[\sum_{i=2}^{k} (q^T M_i q)^{i-1} \Lambda^T M_i q \right] \tag{5}$$

In equation (5), $\bar{R}$ is a positive-definite matrix to be defined later, and $\Lambda = \Lambda(Z)$ is the gradient matrix of $q(Z)$ defined as,

$$\Lambda = \Lambda(Z) = \partial q(Z)/\partial Z \tag{6}$$

The first three terms in the performance index of equation (4) are quadratic performance indices in terms of the non-linear states $q(Z)$, absolute acceleration $\ddot{X}_a(t)$, and the control vector $U(t)$. An optimal non-linear control law, based on such a quadratic performance index of non-linear states $q(Z)$, was presented by Yang *et al.*[8,9] In this paper, we generalize the performance index to include the fourth term, which is the summation of the polynomial of non-linear states $q(Z)$ of different orders higher than the quadratic term. The last term $\bar{h}(q)$ in equation (4) has been added such that simple analytical solutions can be obtained. Weighting matrices Q, R, Q_a and Q_i, $i = 2, 3, \ldots, k$, can be chosen in an arbitrary manner to penalize selected quantities. However, matrices, M_i, $i = 2, 3, \ldots, k$, are implicit functions of the weighting matrices Q_i, $i = 2, 3, \ldots, k$. The relation between M_i and Q_i will be defined later.

Generally, a factor of 1/2 should be multiplied to the performance index in equation (4). However, the optimal solution (or control law) does not depend on any constant factor multipled to the performance index. For simplicity of presentation, the constant factor of 1/2 has been dropped.

Transformed performance index

The penalty on $\ddot{X}_a(t)$ has been included in the performance index, equation (4), in order to reduce the absolute acceleration of each floor to an acceptable level. From the equation of motion, equation (1), the absolute acceleration vector $\ddot{X}_a(t)$ can be expressed as,

$$\ddot{X}_a(t) = -LM^{-1}[F_c(\dot{X}) + F_s(X)] + LM^{-1}HU(t) \tag{7}$$

in which L is an $(n \times n)$ transformation matrix. For a shear-beam type building, $L(i, j) = 1$ for $j \leqslant i$ and $L(i, j) = 0$ for $j > i$. Substituting equation (7) into equation (4), one obtains a transformed performance index as follows:[8]

$$J = \int_0^\infty \left[q^T \bar{Q} q + \bar{U}^T \bar{R} \bar{U} + \sum_{i=2}^{k} (q^T M_i q)^{i-1} q^T Q_i q + \bar{h}(q) \right] dt \tag{8}$$

where $\bar{R}$, $\bar{Q}$ and $\bar{U}$ are

$$\bar{T}_a = \begin{bmatrix} 0 & 0 \\ 0 & L^T Q_a L \end{bmatrix}; \quad \bar{R} = R + B^T \bar{T}_a B; \quad \bar{Q} = Q + \bar{T}_a - \bar{T}_a B \bar{R}^{-1} B^T \bar{T}_a \tag{9}$$

$$\bar{U} = U + \bar{R}^{-1} B^T \bar{T}_a q(Z) \tag{10}$$

Substituting equation (10) into equation (2), one obtains the transformed state equation as

$$\dot{Z} = \bar{A} q + B\bar{U} + E(t) \tag{11}$$

where

$$\bar{A} = [I - B\bar{R}^{-1} B^T \bar{T}_a] \tag{12}$$

The minimization of the performance index in equation (8) by classical conditions of optimality is very difficult and hence an alternative approach has been developed. This approach is based on the solution of the Hamilton–Jacobi–Bellman (H–J–B) equation[26] using a function which is polynomial in terms of nonlinear states $q(Z)$ of the system. This function is required to satisfy all the properties of a Lyapunov function.

Optimality conditions

Let us consider a general time-dependent state equation,

$$\dot{Z}(t) = f(Z, \bar{U}, t); \quad Z(t_0) = Z_0 \tag{13}$$

and a general performance index J as follows,

$$J = J(Z_0, \bar{U}(t), t_0) = S(Z_T, T) + \int_{t_0}^{T} L(Z(t), \bar{U}(t), t)\,dt \tag{14}$$

where $Z_0 = Z(0)$ is the initial state, $Z_T = Z(T)$ is the terminal state, $S(Z_T, T)$ is the terminal cost, and $L(Z(t), \bar{U}(t), t)$ is a general non-negative cost function.

The minimization of $J(Z_0, \bar{U}, t_0)$ for the system in equation (13) results in the well-known Hamilton–Jacobi–Bellman (H–J–B) equation[26]

$$\frac{\partial V(Z)}{\partial t} = -\min_{\bar{U}} [H(Z, \bar{U}, V'(Z), t)] \tag{15}$$

where a prime indicates the differentiation with respect to Z, $V(Z)$ is the optimal cost function, and the Hamiltonian function H is given by

$$H(Z, \bar{U}, V', t) = L(Z, \bar{U}, t) + [V'(Z)]^T f(Z, \bar{U}, t) \tag{16}$$

The necessary condition for the minimization of the right-hand side of equation (15) is

$$\frac{\partial H(Z, \bar{U}, V', t)}{\partial \bar{U}} = \frac{\partial L(Z, \bar{U}, t)}{\partial \bar{U}} + \frac{\partial f(Z, \bar{U}, t)}{\partial \bar{U}} V'(Z) = 0 \tag{17}$$

in which equation (16) has been used. The solution of equation (17) will yield the minimum control $\bar{U}(t) = \phi(Z)$ if $\partial^2 H(Z, \bar{U}, V', t)/\partial \bar{U}^2 \geqslant 0$. For the optimal control, $\bar{U} = \phi(Z)$, obtained from equation (17), the H–J–B equation in equation (15) can be expressed as

$$\frac{\partial V(Z)}{\partial t} + H(Z, \phi(Z), V'(Z), t) = 0 \tag{18}$$

For an optimal cost function $V(Z)$ which satisfies all the properties of a Lyapunov function, if there exists an optimal control $\bar{U} = \phi(Z)$, which satisfies equations (17) and (18), then the closed-loop system is asymptotically stable and the minimum value of the performnce index in equation (14) is obtained as $J(Z_0, \phi(Z), t_0) = V(Z_0)$. Furthermore, the feedback control $\bar{U} = \phi(Z)$ minimizes $J(Z_0, \bar{U}, t_0)$ in the sense that $J(Z_0, \phi(Z), t_0) = \min_{\bar{U} \in \Omega}[J(Z_0, \bar{U}, t_0)]$. The asymptotic stability of the closed-loop system is guaranteed through the Lyapunov theorem of stability, i.e. $\dot{V}(Z) \leqslant 0$.

Derivation of the controller

For non-linear or hysteretic civil engineering structures, such as yielded structural members, rubber bearings, sliding bearings, etc., the initial state $Z = 0$ is the only equilibrium point, that is stable in the open-loop system (without control). In addition, there are infinite numbers of neutral equilibrium points, corresponding to the permanent drift (or deformations), which are also stable in the open-loop system (without control). For the closed-loop system (with control), as long as we can guarantee the stability of the equilibrium point at the initial state $Z = 0$, all the neutral equilibrium points are stable. With this premise, the external disturbance $E(t)$ will not affect the system stability and , hence, it can be neglected in deriving the controller. A comparison of the state equation in equation (11) with the general state equation in equation (13) leads to

$$f(Z, \bar{U}, t) = \bar{A}q(Z) + B\bar{U}(t) \tag{19}$$

Now, we consider a cost function $L(Z, \bar{U})$ and a Lyapunov function $V(Z)$ as follows,

$$L(Z, \bar{U}) = q^T \bar{Q} q + \bar{U}^T \bar{R} \bar{U} + h(q) \tag{20}$$

$$V(Z) = q^T P q + g(q) \tag{21}$$

where $g(q)$ is some positive definite multinomial of q. Our aim is to determine the non-quadratic cost function, $h(q)$, such that a simple analytical solution for the optimal control law $\bar{U}$ can be derived. Substituting equations (19)–(21) into equation (16), one obtains the Hamiltonian function

$$H(q, \bar{U}, V', t) = q^{\mathrm{T}}\bar{Q}q + \bar{U}^{\mathrm{T}}\bar{R}\bar{U} + h(q) + [2q^{\mathrm{T}}P\Lambda + g'(q)^{\mathrm{T}}](\bar{A}q + B\bar{U}) \tag{22}$$

in which the derivative matrix $\Lambda = \Lambda(Z)$ is given by equation (6). Substitution of equation (22) into the necessary condition in equation (17) leads to

$$2\bar{R}\bar{U} + 2B^{\mathrm{T}}\Lambda^{\mathrm{T}}Pq + B^{\mathrm{T}}g'(q)^{\mathrm{T}} = 0 \tag{23}$$

From equation (23), one obtains the optimal non-linear controller, $\bar{U}(t)$, as

$$\bar{U}(t) = -\bar{R}^{-1}B^{\mathrm{T}}\Lambda^{\mathrm{T}}Pq(Z) - \tfrac{1}{2}\bar{R}^{-1}B^{\mathrm{T}}g'(q) \tag{24}$$

It can be verified easily that $\partial^2 H(Z, \bar{U}, V', t)/\partial\bar{U}^2 = 2\bar{R} > 0$, since $\bar{R}$ is a positive-definite matrix. Substituting equations (19)–(21) and equation (24) into the H–J–B equation in equation (18), and separating quadratic terms in q and terms containing $g'(q)$, one obtains

$$-\dot{P} = P\Lambda\bar{A} + \bar{A}^{\mathrm{T}}\Lambda^{\mathrm{T}}P - P\Lambda B\bar{R}^{-1}B^{\mathrm{T}}\Lambda^{\mathrm{T}}P + \bar{Q} \tag{25}$$

$$-\frac{\partial g(q)}{\partial t} = h(q) - \tfrac{1}{4}g'(q)^{\mathrm{T}}B\bar{R}^{-1}B^{\mathrm{T}}g'(q) + g'^{\mathrm{T}}(\bar{A} - B\bar{R}^{-1}B^{\mathrm{T}}\Lambda^{\mathrm{T}}P)q \tag{26}$$

in which the scalar identity $2q^{\mathrm{T}}P\Lambda\bar{A}q = q^{\mathrm{T}}P\Lambda\bar{A}q + q^{\mathrm{T}}\bar{A}^{\mathrm{T}}\Lambda^{\mathrm{T}}Pq$ has been used to obtain equation (25). Equation (25) is the well-known Riccati matrix equation.

To express the controller in equation (24) as an explicit functionale of multinomials in $q(Z)$, we choose $g(q)$ in the following form,

$$g(q) = \sum_{i=2}^{k} \frac{1}{i}(q^{\mathrm{T}}M_i q)^i \tag{27}$$

such that

$$g'(q) = 2\sum_{i=2}^{k} (q^{\mathrm{T}}M_i q)^{i-1}\ \Lambda^{\mathrm{T}}M_i q \tag{28}$$

where k is any integer greater than 2 indicating the order of the multinomials $g(q)$, and the M_i's are positive-definite matrices. Substitution of $g'(q)$ in equation (28) into equation (24) leads to the optimal non-linear controller $\bar{U}$ as

$$\bar{U} = -\bar{R}^{-1}B^{\mathrm{T}}\Lambda^{\mathrm{T}}Pq(Z) - \bar{R}^{-1}B^{\mathrm{T}}\sum_{i=2}^{k}(q^{\mathrm{T}}M_i q)^{i-1}\Lambda^{\mathrm{T}}M_i q(Z) \tag{29}$$

We note that for any value of $k \geqslant 2$, the maximum order of the controller in terms of the non-linear state $q(Z)$ is $(2k + 1)$.

Now, let us choose $h(q)$ in equation (26) as follows,

$$h(q) = \bar{h}(q) + \sum_{i=2}^{k}(q^{\mathrm{T}}M_i q)^{i-1}q^{\mathrm{T}}Q_i q \tag{30}$$

in which $\bar{h}(q) = \bar{h}_1(q)$ is given by equation (5). Substituting equations (27), (28) and (30) into equation (26), one obtains M_i for $i = 2, 3, \ldots, k$, as follows,

$$-\dot{M}_i = M_i\Lambda(\bar{A} - B\bar{R}^{-1}B^{\mathrm{T}}\Lambda^{\mathrm{T}}P) + (\bar{A} - B\bar{R}^{-1}B^{\mathrm{T}}\Lambda^{\mathrm{T}}P)^{\mathrm{T}}\Lambda^{\mathrm{T}}M_i + Q_i \tag{31}$$

Hence, substituting equation (29) into equation (10), we obtain the optimal controller $U(t)$ as

$$U(t) = -\bar{R}^{-1}B^T(\bar{T}_a + \Lambda^T P)q - \bar{R}^{-1}B^T \sum_{i=2}^{k} (q^T M_i q)^{i-1}\Lambda^T M_i q \tag{32}$$

in which $\bar{R}$ and $\bar{T}_a$ are given by equation (9), and positive definite gain matrices P and M_i are obtained by solving the Riccati matrix equation in equation (25) and the Lyapunov matrix equations in equation (31), respectively.

If $\bar{h}(q)$ in equation (30) is chosen to be

$$\bar{h}(q) = \bar{h}_2(q) = \bar{h}_1(q) - \sum_{i=2}^{k} (q^T M_i q)^{i-1}(q^T M_i \Lambda B \bar{R}^{-1} B^T \Lambda^T M_i q) \tag{33}$$

then it follows from equation (26) that the M_i's are determined from the following matrix Riccati equation,

$$-\dot{M}_i = M_i\Lambda(\bar{A} - B\bar{R}^{-1}B^T\Lambda^T P) + (\bar{A} - B\bar{R}^{-1}B^T\Lambda^T P)^T\Lambda^T M_i - M_i\Lambda B\bar{R}^{-1}B^T\Lambda^T M_i + Q_i \tag{34}$$

It is observed from equations (21), (25), (27) and (31) that the function $V(Z)$ satisfies all the properties of the Lyapunov function.

Constant gain matrices

Since the derivative matrix, $\Lambda = \Lambda(Z)$, in equations (25), (31) or (34) is a non-linear function of Z, equation (6), gain matrices P and M_i for the polynomial controller, equation (32), cannot be calculated off-line. Hence, P and M_i will be determined by linearizing $\Lambda(Z)$ at the intial equilibrium point $Z = 0$, which is stable for civil engineering structures. For many civil engineering structures, the stable initial point $Z = 0$ is the only equilibrium point as described previously. With such a premise, we linearize the derivative matrix $\Lambda(Z)$ at $Z = 0$, i.e. $\Lambda_0 = \Lambda(Z)|_{Z=0}$. Replacing $\Lambda(Z)$ by the linearized form at $Z = 0$, i.e. $\Lambda(Z) = \Lambda_0$, one obtains from equations (25), (31) and (34) for the steady-state Riccati and Lyapunov matrix equations, respectively,

$$\hat{P}\Lambda_0\bar{A} + \bar{A}^T\Lambda_0^T\hat{P} - \hat{P}\Lambda_0 B\bar{R}^{-1}B^T\Lambda_0^T\hat{P} + \bar{Q} = 0 \tag{35}$$

$$\hat{M}_i\Lambda_0(\bar{A} - B\bar{R}^{-1}B^T\Lambda_0^T\hat{P}) + (\bar{A} - B\bar{R}^{-1}B^T\Lambda_0^T\hat{P})^T\Lambda_0^T\hat{M}_i + Q_i = 0, \quad i = 2, 3, \ldots, k \tag{36}$$

$$\hat{M}_i\Lambda_0(\bar{A} - B\bar{R}^{-1}B^T\Lambda_0^T\hat{P}) + (\bar{A} - B\bar{R}^{-1}B^T\Lambda_0^T\hat{P})^T\Lambda_0^T\hat{M}_i - \hat{M}_i\Lambda_0 B\bar{R}^{-1}B^T\Lambda_0^T\hat{M}_i + Q_i = 0 \tag{37}$$

in which $\hat{P}$ is the constant Riccati matrix, equation (35), and $\hat{M}_i$ is either a constant Lyapunov matrix, equation (36), or a constant Riccati matrix, equation (37). Consequently, the controller in equation (32) can be written as

$$U(t) = -\bar{R}^{-1}B^T(\bar{T}_a + \Lambda^T\hat{P})q - \bar{R}^{-1}B^T \sum_{i=2}^{k} (q^T\hat{M}_i q)^{i-1}\Lambda^T\hat{M}_i q \tag{38}$$

The optimal controller derived in equation (38) is a polynomial of non-linear states q with gain matrices $\hat{P}$, $\hat{M}_i (i = 2, 3, \ldots, k)$, and $\Lambda = \Lambda(Z)$. $\hat{P}$ and $\hat{M}_i$ are constant gain matrices determined by linearizing Λ at $Z = 0$, equations (35)–(37). However, the gain matrices $\Lambda = \Lambda(Z)$ in the controller, Equation (38), which is the derivative matrix, is a non-linear function of the state Z.

To show that the optimal polynomial controller in equation (38), with constant gain matrices $\hat{P}$ and $\hat{M}_i$ being obtained from equations (35)–(37), stabilizes the non-linear system in equation (2), we invoke Lyapunov's linearization method of stability for nonlinear systems[27] as follows.

The closed-loop non-linear system for the first part of the controller in equation (38) is given by

$$\dot{Z}(t) = f_1[t, Z(t)] = (\bar{A} - B\bar{R}^{-1}B^T\Lambda^T\hat{P})q(Z) + E(t) \tag{39}$$

Based on Lyapunov's linearization method of stability for non-linear systems,[27] the closed-loop non-linear system in equation (39) is stable around $Z = 0$ if its linearized system around $Z = 0$ is stable. Now, the linearized system for equation (39) around $Z = 0$ is given by

$$\dot{Z}(t) = \left[\frac{\partial f_1[t, Z(t)]}{\partial Z}\bigg|_{Z=0}\right] Z = (\bar{A} - B\bar{R}^{-1}B^{\mathrm{T}}\Lambda_0^{\mathrm{T}}\hat{P})\Lambda_0 Z \tag{40}$$

Equation (40) can be shown easily to be stable, since $\hat{P}$ is determined from equation (35). Similarly, the closed-loop non-linear systems for the second part of the optimal controller, equation (38), are given by

$$\dot{Z}(t) = f_i[t, Z(t)] = (\bar{A} - B\bar{R}^{-1}B^{\mathrm{T}}\Lambda^{\mathrm{T}}\hat{P} - B\bar{R}^{-1}B^{\mathrm{T}}\Lambda^{\mathrm{T}}\hat{M}_i)q(Z), \quad i = 2, 3, \ldots, k \tag{41}$$

Linearizing equation (41) around $Z = 0$, one obtains

$$\dot{Z}(t) = (\bar{A} - B\bar{R}^{-1}B^{\mathrm{T}}\Lambda_0^{\mathrm{T}}\hat{P} - B\bar{R}^{-1}B^{\mathrm{T}}\Lambda_0^{\mathrm{T}}\hat{M}_i)\Lambda_0 Z(t) \tag{42}$$

which is stable, since $\hat{M}_i$ is determined from equation (36) or (37). Consequently, the closed-loop non-linear systems in equations (39) and (41) are stable around the equilibrium point Z = 0. Again the description of stability is based on the premise that $Z = 0$ is the only equilibrium point as described previously. Hence, the local stability of the optimal polynomial controller in equation (38) around Z = 0 also implies the global stability.

The stability of the closed-loop non-linear system in equation (2) around the equilibrium point $Z = 0$, for the controller in equation (38), is equivalent to the stability of the closed-loop non-linear systems in equations (39) and (41) around $Z = 0$. Since the closed-loop non-linear systems in equations (39) and (41) have been proved to be stable, the controller in equation (38) stabilizes the non-linear system in equation (2).

The controller derived above holds for general non-linear structures. For special types of non-linear (or hysteretic) structures, in which the dampings and stiffnesses consist of linear and non-linear parts, the formulation of the controller is given in Appendix I. Such a controller reduces directly to that presented by Agrawal and Yang[23,24] for linear structures. Likewise, the formulation of the controller in Appendix I can be extended to the static output feedback controller.[28,29]

RESPONSE OF HYSTERETIC STRUCTURES

In order to evaluate the effectiveness and performance of the optimal polynomial controller, simulations for the response of the controlled structure will be conducted. Suppose the non-linearity for both the structure and passive protective systems is reflected by the stiffness restoring force $F_s[X(t)]$ in equation (1) and the damping is linear, i.e. $F_c[\dot{X}(t)] = C\dot{X}$, where C is an $(n \times n)$ damping matrix. The ith element, $F_{si}(x_i)$, of the vector $F_s[X(t)]$ is modelled as[8]

$$F_{si}[x_i(t)] = \alpha_i k_i x_i + (1 - \alpha_i)k_i D_{yi} v_i \tag{43}$$

in which k_i is the elastic stiffness of the ith storey unit, α_i is the ratio of the post-yielding to pre-yielding stiffness, D_{yi} is the yield deformation = constant, and v_i is the non-dimensional hysteretic component of the deformation, with $|v_i| \leqslant 1$, where

$$\dot{v}_i = D_{yi}^{-1}[A_i\dot{x}_i - \beta_i|\dot{x}_i||v_i|^{n_i-1}v_i - \gamma_i\dot{x}_i|v_i|^{n_i}] = f_i(\dot{x}_i, v_i) \tag{44}$$

In equation (44), A_i, β_i, γ_i and n_i are parameters characterizing the hysteresis loop of the inelastic behaviour of the ith storey unit. Substituting equation (43) into equation (1) with $F_c(\dot{X}) = C\dot{X}$, one obtains the vector equation of motion as follows,

$$M\ddot{X} + C\dot{X} + K_e X(t) + K_I \bar{V}(t) = HU(t) + \eta\ddot{X}_0(t) \tag{45}$$

where K_e and K_I are the elastic and inelastic stiffness matrices, assembled for each storey unit according to equation (43); $\bar{V}(t) = [v_1, v_2, \ldots, v_n]^{\mathrm{T}}$ is an n-vector denoting the hysteretic component of each storey unit

given by equation (44). The derivative matrices $\Lambda(Z)$ and $\Lambda_0 = \Lambda(Z)|_{Z=0}$ appearing in the control law equations (35)–(38), are given by

$$\Lambda(Z) = \begin{bmatrix} 0_{nn} & I_{nn} \\ -M^{-1}\left[K_e + K_1 \dfrac{\partial \bar{V}}{\partial X}\right] & -M^{-1}C \end{bmatrix}; \quad \Lambda_0 = \begin{bmatrix} 0_{nn} & I_{nn} \\ -M^{-1}K_e & -M^{-1}C \end{bmatrix} \tag{46}$$

in which 0_{nn} and I_{nn} are $(n \times n)$ null and identity matrices, respectively, and $\partial \bar{V}/\partial X$ is a diagonal matrix with the ith diagonal element $\partial v_i/\partial x_i$ given by

$$\frac{\partial v_i}{\partial x_i} = \frac{\partial \dot{v}_i}{\partial \dot{x}_i} = D_{yi}^{-1}[A_i - \beta_i \operatorname{sgn}(\dot{x}_i)|v_i|^{n_i-1}v_i - \gamma_i|v_i|^{n_i}] \tag{47}$$

The linearized constant matrix Λ_0, which is required for the calculation of the feedback gain matrices in equations (35)–(37), is obtained from $\Lambda(Z)$ by setting $Z = 0$ or $\partial \bar{V}/\partial X = 0$ in equation (46). For numerical simulations of the structural response, the hysteretic vector $\bar{V}$ can be augmented in equations (44) and (45) so that the state vector $Z = [X^T, \dot{X}^T, \bar{V}^T]^T$, has a $3n$ dimension. A detailed description of the procedures for numerical simulations of the response of hysteretic structures can be found in Yang *et al.*[8]

OTHER CONTROL LAWS FOR NON-LINEAR OR HYSTERETIC STRUCTURES

The performance of the controller presented in this paper will be compared with some other controllers available in the literature. These control methods include the LQR method based on linearized structures, the non-linear controller presented by Yang et al.,[8,9] and the continuous sliding mode controller[12–14] to be described briefly in the following.

Non-linear controller: If we choose the weighting matrices $Q_i = 0$ for $i = 2, 3, \ldots, k$ in the performance index given by equation (4), then the controller in equation (38) becomes $U(t) = -\bar{R}^{-1}B^T(\bar{T}_a + \Lambda^T\hat{P})q$. This special non-linear controller, consisting of only the first term of our polynomial controller, was proposed by Yang *et al.*[8,9]

LQR with acceleration penalty: If the non-linear or hysteretic structure is linearized first at the equilibrium point $Z = 0$, the linearized state equation becomes $\dot{Z} = \Lambda_0 Z(t) + BU(t) + E(t)$. Then, for the quadratic performance index

$$J = \int_0^\infty [Z^T Q Z + \ddot{X}_a^T Q_a \ddot{X}_a + U^T R U]\, dt \tag{48}$$

the linear optimal control law is obtained as

$$U(t) = -\bar{R}^{-1}B^T(\bar{T}_a + P)Z(t) \tag{49}$$

where P is an appropriate Riccati matrix (see Yang *et al.*[8] for details).

Sliding mode control: The method of sliding mode control was developed for robust control of uncertain non-linear systems. Applications of continuous sliding mode control, which has no undesirable chattering effect, to civil engineering structures was presented by Yang *et al.*[12–19] In this approach, a sliding surface

$$S = \bar{P}Z(t) = 0 \tag{50}$$

is designed such that the motion on the sliding surface is stable. In equation (50), $S = [S_1, S_2, \ldots, S_r]^T$ is an r-vector consisting of sliding variables S_i, where r is the total number of controllers, and $\bar{P}$ is a $(r \times 2n)$ matrix to be determined either by the method of pole assignment or the classical LQR method. The designs of various controllers were given in Yang *et al.*[12,13]

NUMERICAL SIMULATIONS

To demonstrate the performance of the optimal polynomial controller, numerical simulations have been conducted for an elasto-plastic eight-storey building either with a fixed-base or with a hybrid control system consisting of rubber-bearing isolators and actuators, Figure 1. The performance of the proposed controller will be compared with that of various controllers described previously.

Example 1: A base-isolated elasto-plastic building

An eight-storey building that exhibits bilinear elasto-plastic behaviour is considered. The properties of the building are as follows: (i) the mass of each floor is identical with $m_i = 345{\cdot}6$ metric tons; (ii) pre-yielding stiffnesses k_i ($i = 1, 2, \ldots, 8$) of eight-storey units are 340 400, 325 700, 284 900, 268 600, 243 000, 207 300, 168 700 and 136 600 kN/m, respectively, and post-yielding stiffnesses are $0{\cdot}1k_i$ for $i = 1, 2, \ldots, 8$, i.e., $\alpha_i = 0{\cdot}1$ in equation (43); and (iii) the linear viscous damping coefficients for each storey unit are $c_i = 490$, 467, 410, 386, 348, 298, 243 and 196 kN s/m, respectively. The damping coefficients result in a damping ratio of 0·38 per cent for the first vibrational mode. The fundamental frequency of the unyielded building is 5·24 rad/s. The yielding level for each storey unit varies with respect to the stiffness; with the results, $D_{yi} = 2{\cdot}4$, 2·3, 2·2, 2·1, 2·0, 1·9, 1·7 and 1·5 cm, equation (44). The bilinear elasto-plastic behaviour can be described by the hysteretic model, equation (44), with $A_i = 1{\cdot}0$, $\beta_i = 1{\cdot}0$, $n_i = 95$ and $\gamma_i = 1{\cdot}0$ for $i = 1, 2, \ldots, 8$. The El Centro NS (1940) earthquake with a peak ground acceleration of $0{\cdot}3g$, referred to as the design earthquake as shown in Figure 2, is used for the input excitation.

Without any control system, it has been observed that the deformation of the unprotected building is excessive and that yielding takes place in the upper five storey.[6,8] Hence, a lead-core rubber bearing isolation system is used to reduce the response of the building. The stiffness of the lead-core rubber bearing is modelled by equation (43) with $F_{sb} = \alpha_b k_b x_b + (1 - \alpha_b) k_b D_{yb} v_b$ in which the subscript b stands for the base-isolation system. The hysteretic component, v_b, is modelled by equation (44). Properties of the base-isolation system are: $m_b = 450$ metric tons, stiffness $k_b = 18\,050$ kN/m, damping $c_b = 26{\cdot}17$ kN s/m, $\alpha_b = 0{\cdot}6$, $D_{yb} = 4$ cm,

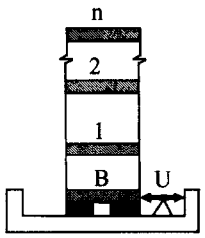

Figure 1. A base-isolated structural model

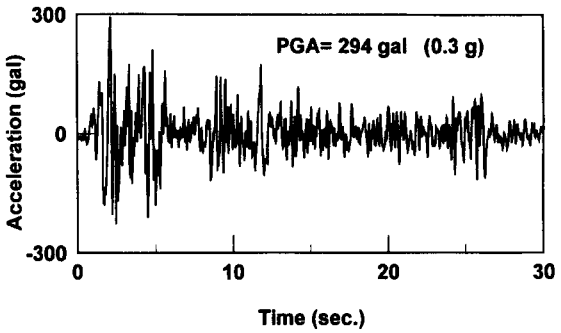

Figure 2. El Centro earthquake (NS component)

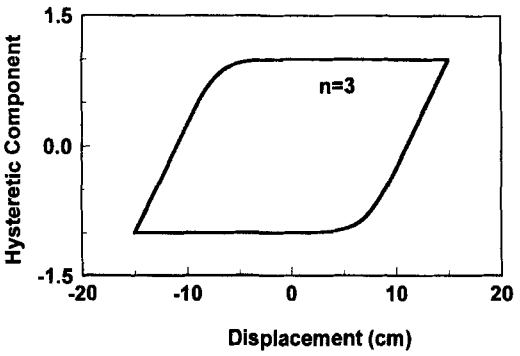

Figure 3. Hysteresis loop of lead-core rubber bearings

$A_b = 1{\cdot}0$, $\beta_b = 0{\cdot}5$, $n_b = 3$ and $\gamma_b = 0{\cdot}5$, equation (44). The hysteresis loop of such a base-isolation system, i.e. x_b versus v_b, is shown in Figure 3.

For the building with the base-isolation system, the first natural frequency of the pre-yielded structure is 2·21 rad/s and the damping ratio for the first vibrational mode is 0·16 per cent. Within 30 s of the earthquake episode, the peak interstorey drifts, x_i, and peak absolute accelerations, $\ddot{x}_{ai}$, of different floors of the base-isolated building are shown in columns (3) and (4) of Table I, designated as 'With BIS'. The results of x_b and $\ddot{x}_b$ for rubber bearings are shown in the row denoted by B. It is observed from Table I that the interstorey drifts are within the elastic range. However, the peak drift of the base-isolation system is excessive and should be reduced.

Sliding mode control

In order to reduce the drift of the base-isolation system, actuators are attached to the base isolation system, referred to as the hybrid control system, as shown in Figure 1. We first consider the use of sliding mode control presented by Yang *et al.*[12, 13] The sliding surface $\bar{P}$ in Equation (50) is a row vector with $\bar{P} = [\bar{P}_1, \bar{P}_2]$ and it is designed as follows,

$$\bar{P}_1 = [0{\cdot}0707 \quad -90{\cdot}533 \quad -49{\cdot}462 \quad 2{\cdot}919 \quad 10{\cdot}396 \quad 7{\cdot}596 \quad 3{\cdot}053 \quad 3{\cdot}340 \quad 1{\cdot}796]$$

$$\bar{P}_2 = [0{\cdot}795 \quad -0{\cdot}205 \quad -3{\cdot}054 \quad -3{\cdot}198 \quad -2{\cdot}518 \quad -1{\cdot}859 \quad -1{\cdot}423 \quad -0{\cdot}974 \quad -0{\cdot}474]$$

The controller in equation (6.19) of Yang *et al.*[12] with $\delta_1 = 5 \times 10^5$ kN.ton.cm/s is used. The peak interstorey drifts and absolute floor accelerations are shown in columns (13) and (14) of Table I, designated as 'Sliding Mode'. Also shown in Table I is the peak control force U that is expressed in terms of the percentage of the total building weight. The total building weight is 3 214·8 metric tons. The required control effort (energy) $\overline{U^2}$ which is the integral of the square of the control force $U(t)$ over the duration of 30 s of the earthquake episode, is also shown in Table I. We observe that sliding mode control is very effective in reducing the response quantities of the entire system. In particular, the drift of rubber bearings has been reduced by 49 per cent.

Linear control

Next, we consider the LQR control law, equation (49), in which the structural system is linearized first at $Z = 0$. Two cases of weighting matrices for this controller have been considered. In the first case, we choose the scalar control weighting matrix $R = 7{\cdot}3 \times 10^{-10}$, and all elements of Q and Q_a are zero except $Q_a(1,1) = 200$ and $Q(1,1) = 78$. The peak response quantities are shown in columns (5) and (6) of Table I, designated as 'Linear 1'. These weighting matrices have been chosen such that the peak response quantities and the peak control force are as close as possible to those associated with the sliding mode controller. It is

Table I. Peak response quantities of an eight-storey building equipped with a hybrid control system

		With BIS		Linear 1 $U = 1491$ kN (4·73%) $\overline{U^2} = 1047$ kN^2		Linear 2 $U = 1031$ kN (3·27%) $\overline{U^2} = 226$ kN^2		Nonlinear 1 $U = 1437$ kN (4·56%) $\overline{U^2} = 689$ kN^2		Nonlinear 2 $U = 1350$ kN (4·29%) $\overline{U^2} = 711$ kN^2		Sliding Mode $U = 1494$ kN (4·74%) $\overline{U^2} = 651$ kN^2	
Floor no. (1)	D_y (cm) (2)	x_i (cm) (3)	$\ddot{x}_{ai}$ (cm/s^2) (4)	x_i (cm) (5)	$\ddot{x}_{ai}$ (cm/s^2) (6)	x_i (cm) (7)	$\ddot{x}_{ai}$ (cm/s^2) (8)	x_i (cm) (9)	$\ddot{x}_{ai}$ (cm/s^2) (10)	x_i (cm) (11)	x_{ai} (cm/s^2) (12)	x_i (cm) (13)	x_{ai} (cm/s^2) (14)
B	4·0	21·35	130	14·4	45	10·7	70	10·7	38	10·7	46	10·8	77
1	2·4	0·62	123	0·15	43	0·22	71	0·20	39	0·18	48	0·14	42
2	2·3	0·59	113	0·16	40	0·25	66	0·20	36	0·18	43	0·14	37
3	2·2	0·65	111	0·19	33	0·29	53	0·22	30	0·21	34	0·16	38
4	2·1	0·63	102	0·21	29	0·30	46	0·23	30	0·22	30	0·15	31
5	2·0	0·65	91	0·22	32	0·30	49	0·22	38	0·21	40	0·14	38
6	1·9	0·65	103	0·23	39	0·31	66	0·22	46	0·20	46	0·18	39
7	1·7	0·60	135	0·22	50	0·34	68	0·20	47	0·20	51	0·20	42
8	1·5	0·41	163	0·16	64	0·27	105	0·15	60	0·16	64	0·15	60

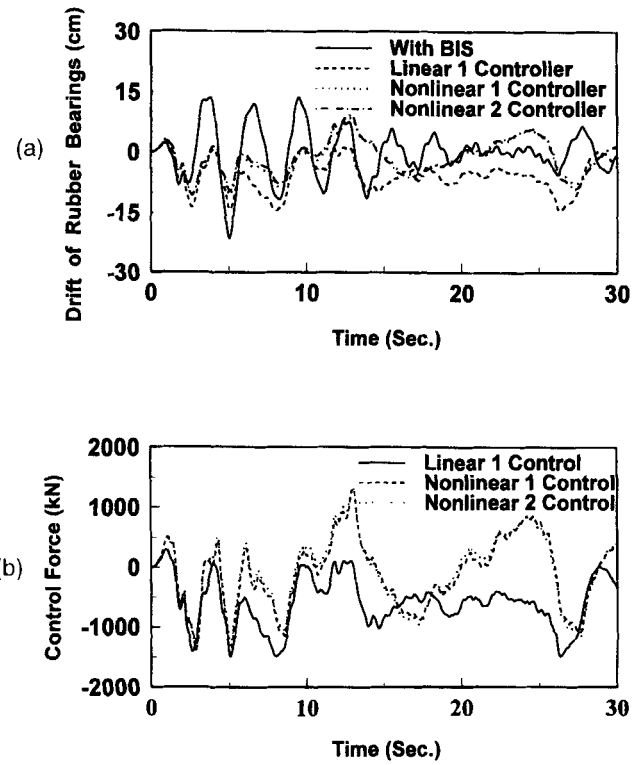

Figure 4. Time-histories of responses and control forces: (a) drift of rubber bearings; (b) control forces

observed that the drift of the rubber bearing and the required control effort $\overline{U^2}$ are larger than that based on the sliding mode controller. To emphasize more on the reduction of the drift of the rubber bearing, non-zero elements of the weighting matrices are chosen to be $Q_a(1,1) = 10$ and $Q(1,1) = 130$ for the second case. With $R = 7{\cdot}3 \times 10^{-11}$, the peak response quantities are presented in columns (7) and (8), respectively, of Table I, designated as 'Linear 2'. It is observed that, although the drift of the rubber bearing and the peak control force are reduced, the building response quantities increase.

Optimal polynomial control

For the controller, equation (38), presented in this study, we first consider the special case in which $Q_i = 0$, $i = 2, 3, \ldots, k$. Such a special controller was proposed by Yang *et al.*[8,9] In this case, we choose $R = 1{\cdot}0 \times 10^{-7}$, and Q_a and Q are diagonal matrices as follows: $Q_a(i,i) = [10, 15, 15, 20, 20, 30, 50, 50, 50]$, $Q(1,1) = 100$, $Q(i,i) = 10$ for i = 2, 3, ..., 9, and $Q(i,i) = 0$ for $i = 10, 11, \ldots, 18$. The peak response quantities based on this controller are shown in columns (9) and (10) of Table I, designated as 'Non-linear 1'. We observe that the overall performance of this controller is slightly better than that of linear controllers. Next, we consider a general case, where $Q_2 \neq 0$ and $Q_i = 0$ for $i = 3, 4, \ldots, k$. Diagonal weighting matrices are chosen as follows: $R = 1{\cdot}0 \times 10^{-4}$, $Q_a(i,i) = [4, 6, 6, 8, 8, 12, 35, 35, 35] \times 10^3$, $Q(1,1) = 2$, $Q(i,i) = 1$ for $i = 2, 3, \ldots, 9$, $Q(i,i) = 0$ for $i = 10, 11, \ldots, 18$, $Q_2(1,1) = 8$, $Q_2(i,i) = 6$ for $i = 2, 3, \ldots, 6$, $Q_2(i,i) = 1$ for $i = 7, 8, 9$ and $Q_2(i,i) = 0$ for $i = 10, 11, \ldots, 18$. The peak response quantities based on this controller are shown in columns (11) and (12) of Table I, designated as 'Non-linear 2'. It is observed that, while the overall performance is similar to that of 'Non-linear 1', the peak control force has been decreased by 5 per cent. In particular, the overall performance of 'Non-linear Controller 2' is comparable with that of the sliding mode controller.

Time histories for the drift of rubber bearings are shown in Figure 4(a), in which the response without actuator is shown by the solid curve. The dashed, dotted and dashed-dotted curves represent the responses

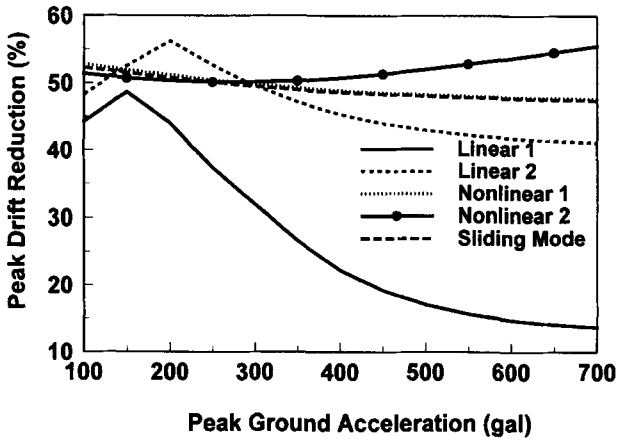

Figure 5. Peak drift reduction of rubber bearings vs. peak ground acceleration

using Linear1, Non-linear 1 and Non-linear 2 controllers, respectively. The required control forces for these controllers are shown in Figure 4(b). As observed from Figure 4 and Table 1, hybrid control is quite effective and the performances of both Non-linear 1 and Non-linear 2 controllers are comparable.

Variation of peak ground acceleration

With hybrid control, the building response quantities are well within the elastic range except the drift of rubber bearings. Hence, the reduction for the drift of rubber bearings will be compared for different controllers in the following. The results presented in Table I are based on the design earthquake, i.e. the El Centro earthquake with a peak ground acceleration (PGA) of 0·3 g. Since the PGA is stochastic in nature, numerical simulations have been conducted for the same earthquake with different PGA. Based on the same design for various controllers presented in Table I, simulation results for the percentages of reduction for the peak drift of rubber bearings as a function of PGA are shown in Figure 5. The peak drift reduction in per cent shown in Figure 5 is defined as $(x^* - x)/x^*$ where x^* and x are the peak drifts without and with active control. It is observed from Figure 5 that, for the PGA greater than 0·3 g (design earthquake), the peak drift reduction in per cent for linear controllers decreases with the increase of PGA. However, the peak drift reductions for both Non-linear 1 and sliding mode controllers remain almost constant with the increase of PGA. On the other hand, the peak drift reduction for Non-linear 2 increases as the PGA increases. Because of such a load-adaptive property, Non-linear 2 controller is more effective in limiting the peak response of rubber bearings under strong earthquakes. It should be mentioned, however, that the trend for the peak response reduction for the superstructure is quite different from that for rubber bearings. In fact, as PGA increases, the percentage of the peak response reduction for the superstructure decreases for Non-linear 2 controller, whereas it increases for Linear 1 controller. Since the response quantities of the superstructure are well within the elastic range, they are not presented.

The corresponding peak control force, U, and the required control energy, $\overline{U^2}$, are presented in Figures 6 and 7, respectively. These quantities have been normalized, respectively, by the corresponding results for Linear 1 controller subjected to a 700 gal of PGA input. As observed from Figures 6 and 7, the peak control force and the control energy required by all the controllers in Table I are almost the same except for the Linear 1 controller. These quantities are significantly higher for the Linear 1 controller. The advantages of the proposed optimal polynomial controller, in terms of the peak response reduction for rubber bearings, peak control force and required control energy, are demonstrated in Figures 5–7.

Example 2: An elasto-plastic building with active bracing system

The same eight-storey elasto-plastic building considered in Example 1 is subjected to the same El Centro earthquake with a PGA of 1g. However, instead of using a rubber-bearing isolation system, an active bracing

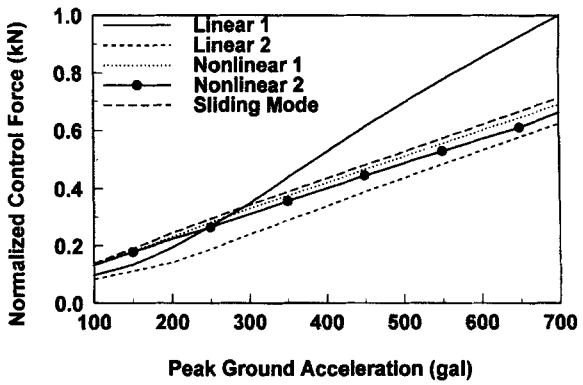

Figure 6. Normalized peak control force vs. peak ground acceleration

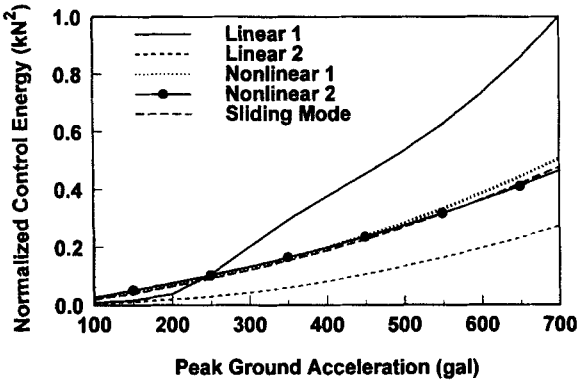

Figure 7. Normalized control energy vs. peak ground acceleration

system is installed on every floor. Hence, the dimensions of weighting matrices Q, Q_a and R are (16×16), (8×8) and (8×8), respectively. Within 30 s of the earthquake episode, the peak interstorey drifts for the uncontrolled structure are presented in column (3) of Table II. It is observed that all the storey units of the building have yielded. In particular, the ductilities of the fifth, sixth and seventh storey units are very large. Hence, it is important to install controllers at every floor to apply control forces effectively.

Linear control

The objective for the control design is to prevent a collapse of the building by reducing the ductility of each storey unit to be smaller than 2·5 cm. We first consider the LQR control law, equation (49), in which the structural system is linearized first at $Z = 0$. In this case, we choose $R(i, i) = 5{\cdot}0 \times 10^{-5}$, $i = 1, 2, \ldots, 8$, $Q_a(i, i) = 0{\cdot}1$, $i = 1, 2, \ldots, 8$ and $Q(i, i) = [15, 16, 22, 18, 15, 11, 6, 1, 0, 0, 0, 0, 0, 0, 0, 0] \times 10^3$. All other elements of the matrices above are zero. The peak interstorey drifts and the peak control force for each controller are shown in columns (4) and (5), respectively, of Table II, designated as 'Linear Control'. Also shown in the table are the maximum of peak control forces, U_{max}, and the maximum required control energy, $\overline{U^2}$, among all actuators. The maximum control force, U_{max}, has also been expressed in parenthesis as the percentage of the total building weight that is 2764·8 metric tons. The peak Control force is about 20·21 per cent because the earthquake has a PGA of $1g$.

Table II. Peak response quantities of a fixed-base eight-storey building under 1g El Centro earthquake

		Without Control	Linear Control U_{max} = 5475 kN (20·21%) $\overline{U^2}$ = 5608 kN^2		Nonlinear Control 1 U_{max} = 4966 kN (18·33%) $\overline{U^2}$ = 5368 kN^2		Nonlinear Control 2 U_{max} = 5192 kN (19·16%) $\overline{U^2}$ = 5510 kN^2		Nonlinear Control 3 U_{max} = 5683 kN (20·97%) $\overline{U^2}$ = 5989 kN^2	
Floor no. (1)	D_y (cm) (2)	x_i (cm) (3)	x_i (cm) (4)	u_i (kN) (5)	x_i (cm) (6)	u_i (kN) (7)	x_i (cm) (8)	u_i (kN) (9)	x_i (cm) (10)	u_i (kN) (11)
1	2·4	4·88	4·35	4961	4·32	4966	4·25	5192	4.32	5683
2	2·3	4·10	4·36	4893	4·35	4803	4.26	5010	4·30	5451
3	2·2	5·38	4·24	5475	4·36	4911	4·28	5068	4·32	5428
4	2·1	5·47	4.21	4613	4·29	4345	4·23	4438	4·08	4731
5	2·0	6·87	3·97	4013	4.09	3853	3·98	3891	3·72	4098
6	1·9	8·48	3·79	3355	3·86	3358	3·65	3372	3·22	3502
7	1·7	10·64	3·82	2303	3·60	2617	3·80	2441	2·79	2542
8	1·5	4·61	3.65	573	3·69	1306	3·53	1212	3·50	1231

Optimal polynomial control

For the polynomial controller, we consider the case when $Q_i = 0$, $i = 2, 3, \ldots, k$. The diagonal weighting matrix Q is chosen as $Q(i,i) = [15{\cdot}3, 15{\cdot}5, 17{\cdot}6, 16{\cdot}1, 14{\cdot}2, 11{\cdot}9, 9, 3{\cdot}3, 0, 0, 0, 0, 0, 0, 0, 0] \times 10^3$, whereas weighting matrices R and Q_a are the same as the linear controller above. The peak interstorey drifts and the peak control forces are shown in columns (6) and (7), respectively, of Table II, designated as 'Non-linear Control 1'. It is observed that the peak control force and the maximum required energy are smaller than those of the linear controller for a similar response reduction of the building. Next, we consider a general case, where $Q_2 \neq 0$ and $Q_i = 0$ and for $i = 3, 4, \ldots, k$. The weighting matrices Q_a, R and Q are kept to be the same as in the case of Non-linear Control 1, except that $Q(7,7) = 7000$ and $Q(8,8) = 2500$. Q_2 is chosen to be a diagonal matrix with diagonal elements $Q_2(i,i) = [0{\cdot}9, 0{\cdot}9, 0{\cdot}9, 0{\cdot}8, 0{\cdot}8, 0{\cdot}8, 0{\cdot}8, 0{\cdot}5, 0, 0, 0, 0, 0, 0, 0, 0]$. The peak interstorey drifts and the peak control forces are shown in columns (8) and (9), respectively, of Table II, designated as 'Non-linear Control 2'. It is observed from Table II that the performance of both non-linear controllers is slightly better than that of the linear controller. A comparison between the results for both non-linear controllers indicates that a slightly better reduction for the interstorey drifts is achieved by Non-linear Control 2 at the expense of increased peak control force and control energy.

Now, we design another controller by increasing the weighting matrix Q_2 for the Non-linear Control 2: $Q_2(i,i) = 1{\cdot}5$, $i = 1, 2, \ldots, 7$, $Q_2(8,8) = 0{\cdot}5$ and $Q_2(i,i) = 0$, $i = 9, 10, \ldots, 16$. The peak interstorey drifts and the peak control forces are shown in columns (10) and (11), respectively, of Table II, designated as 'Non-linear Control 3'. It is noted that the peak control force (20·97 per cent of the building weight) and the maximum control energy have increased slightly as compared with other controllers. However, the maximum ductilities for most critical storey units, i.e. 6th, 7th and 8th storey units, have been reduced significantly.

Variation of peak ground acceleration

Based on the design of various controllers presented in Table II for the 1g earthquake, numerical simulations have been conducted for PGAs in the range of 0·7g to 1·2g to obtain the percentage of reduction for peak interstorey drifts, the peak control force and the maximum control energy as a function of PGA. The results are shown in Figures 8 and 9. Figure 8(a) shows the peak drift reduction for the first storey unit. It is observed that the performance of all the controllers is similar for the whole range of PGA. The peak drift

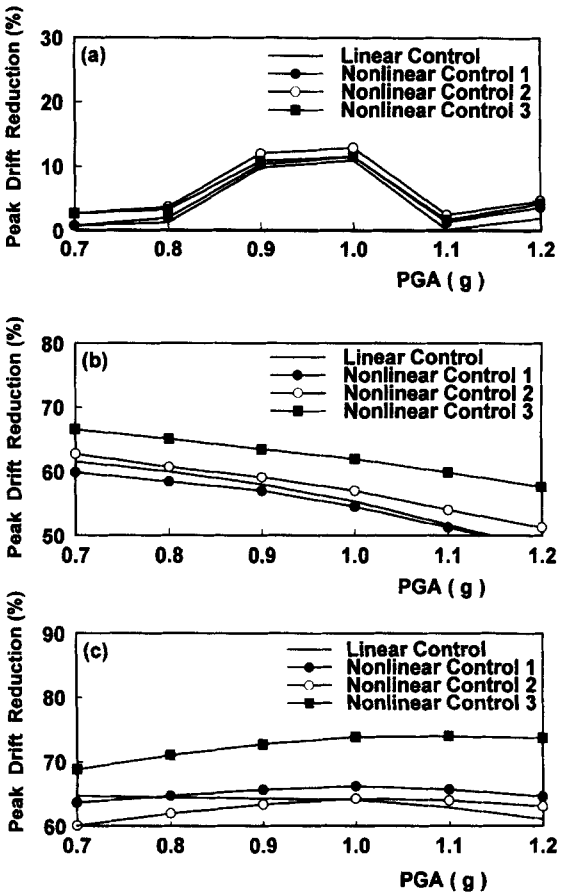

Figure 8. Peak drift reduction of storey units vs. peak ground acceleration; (a) 1st storey unit; (b) 6th storey unit, and (c) 7th storey unit

reduction for the 2nd and 3rd storey units have a similar trend and hence plots are not shown. Figures 8(b) and 8(c) show the peak drift reductions for the 6th and 7th storey units, which are most critical from the safety standpoint as observed from Table II. It is observed from these figures that the peak drift reduction for the Non-linear Control 3 is better than all other controllers for PGA greater than 0·7g. The maximum peak control force, U_{max}, and the required control energy, $\overline{U^2}$, are presented in Figure 8. These quantities have been normalized, respectively, by the corresponding results for the Linear controller subjected to a PGA of 1·2g (i.e. $U_{max} = 6183{\cdot}8$ kN and $\overline{U^2} = 7317{\cdot}6$ kN^2)). For PGA smaller than 0·7 g, both the peak control force and the required control energy are almost the same for all the controllers.

Further extensive simulation results indicate that the peak control force required to drive the system response into the elastic region is approximately 42·8 per cent of the building weight at 1g earthquake. As shown in the Table II, the peak control force is approximately 20 per cent of the building weight in order to reduce the ductility to be smaller than 2·5. Another interesting observation from extensive simulation results is that the percentage of reduction for all interstorey drifts is quite significant for small to moderate earthquakes (PGA $< 0{\cdot}6\,g$).

Numerical simulations were also conducted by solving matrices $\hat{M}_i$, $i = 2, 3 \ldots$, k, using the Riccati matrix equation in equation (37). The results are similar to those obtained by solving the Lyapunov equation, equation (36). Further, results obtained by using the optimal polynomial controller in equation (57) of Appendix I are the same as those obtained by using the controller in equation (38) for appropriate choices of weighting matrices.

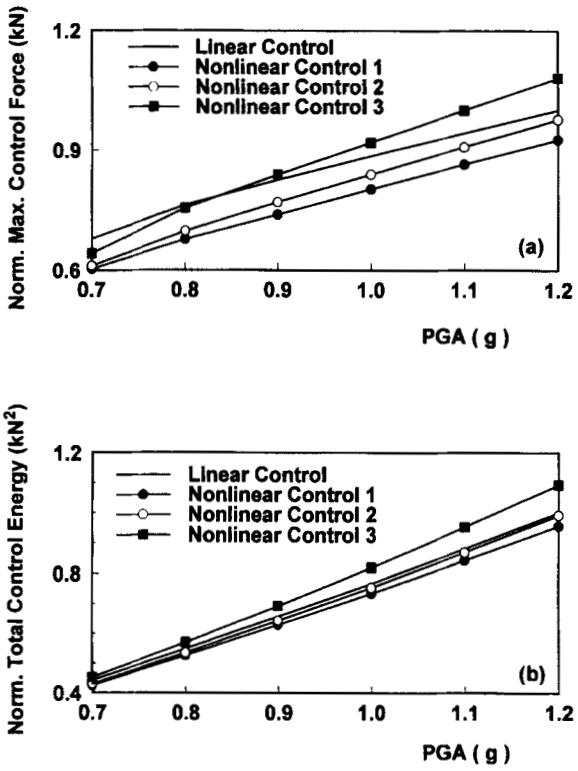

Figure 9. Normalized maximum control force and control energy vs. peak ground acceleration: (a) maximum control force, and (b) control energy

Finally, extensive simulation results using higher-order control laws (higher than the cubic order considered in both examples above) have been obtained. However, their performances are not as good as that of the cubic-order controller, in the sense that for the same level of the peak response reduction, these higher-order control laws require a bigger peak control force and a larger control energy. In fact, the performance for different orders of control laws depends heavily on the nature of non-linearity of the structure considered. For the hysteretic-type non-linearity considered in both examples above (i.e. hysteretic rubber bearings and yielded building), the cubic control law has the best performance.

CONCLUSIONS

An optimal polynomial controller is presented for the peak response control of seismically excited non-linear or hysteretic structures. A performance index, which is quadratic in control and polynomial of any order of non-linear states, is minimized based on the solution of the Hamilton–Jacobi–Bellman equation using a polynomial function of non-linear states, which satisfies all the properties of a Lyapunov function. The resulting optimal controller is polynomial in non-linear states of the system. Gain matrices for different parts of the controller are computed easily by solving Riccati and Lyapunov matrix equations.

Numerical simulations have been conducted for (i) a fixed-base elasto-plastic eight-storey building subjected to a strong earthquake, and (ii) the same building equipped with a hybrid control system consisting of actuators and lead-core rubber bearings. Simulation results indicate that the performance of the optimal polynomial controller presented is quite reasonable. For the building equipped with a hybrid control system, the main advantage of such a controller is its ability to increase the percentage of reduction for the peak response of rubber bearings with the increase of the earthquake intensity. Such a load-adaptive capability is

very desirable in protecting the base-isolation system, in particular when the magnitude of earthquakes exceeds the design one. For the fixed-base elasto-plastic building subjected to a $1g$ design earthquake, the purpose of control is to prevent a catastrophic failure by reducing the ductility of the building to be smaller than 2·5. Simulation results indicate that the optimal polynomial controller presented has a slightly better capability than the linear controller for reducing the building ductility. The optimal polynomial controller is a viable control strategy for seismically excited non-linear and hysteretic civil engineering structures, and it is an addition to available control methods in the literature.

ACKNOWLEDGMENT

This research is supported by the National Science Foundation through grant number CMS-96-25616 and the National Center for Earthquake Engineering Research, NCEER-95-5104B.

APPENDIX I

Special optimal polynomial controller

For most civil engineering structures, such as inelastic or hysteretic structures, the non-linear damping and stiffnesses can be separated into linear and non-linear parts as follows,

$$F_c[\dot{X}(t)] = C\dot{X}(t) + F_{nc}; \quad F_s[X(t)] = KX(t) + F_{ns} \tag{51}$$

in which C and K are $(n \times n)$ linear damping and stiffness matrices, respectively, and $F_{nc} = F_{nc}[\dot{X}(t)]$ and $F_{ns} = F_{ns}[X(t)]$ are n-vectors representing the non-linear parts. Thus, the state equation of the system can be expressed as

$$\dot{Z}(t) = A\bar{q}(Z) + BU(t) + E(t) \tag{52}$$

in which $\bar{q}(Z) = A^{-1}q(Z)$ is the non-liner state vector given by

$$\bar{q}(Z) = Z + A^{-1}\tilde{f}(Z) \tag{53}$$

where $\tilde{f}(Z)$ is the non-linear part of $\bar{q}(Z)$,

$$A = \begin{bmatrix} 0 & I \\ -M^{-1}K & -M^{-1}C \end{bmatrix}; \quad \tilde{f}(Z) = \begin{bmatrix} 0 \\ -M^{-1}[F_{nc} + F_{ns}] \end{bmatrix} \tag{54}$$

For the performance index in equation (4) with q being replaced by $\bar{q}$, one has

$$J = \int_0^\infty \left[\bar{q}^T Q \bar{q} + \ddot{X}_a^T Q_a \ddot{X}_a + U^T R U + \sum_{i=2}^{k} (\bar{q}^T M_i \bar{q})^{i-1} \bar{q}^T Q_i \bar{q} + \bar{h}(\bar{q}) \right] dt \tag{55}$$

where $\bar{h}(\bar{q}) = \bar{h}_1(\bar{q})$ is given by equation (5) with q being replaced by $\bar{q}$, i.e.

$$\bar{h}(\bar{q}) = \bar{h}_1(\bar{q}) = \left[\sum_{i=2}^{k} (\bar{q}^T M_i \bar{q})^{i-1} \bar{q}^T M_i \Lambda \right] B \bar{R}^{-1} B^T \left[\sum_{i=2}^{k} (\bar{q}^T M_i \bar{q})^{i-1} \Lambda^T M_i \bar{q} \right] \tag{56}$$

Following the same derivations, the optimal controller is obtained as

$$U(t) = -\bar{R}^{-1} B^T (\bar{T}_a + \Lambda^T \hat{P}) \bar{q} - \bar{R}^{-1} B^T \sum_{i=2}^{k} (\bar{q}^T \hat{M}_i \bar{q})^{i-1} \Lambda^T \hat{M}_i \bar{q} \tag{57}$$

where $\bar{T}_a$ and $\bar{R}$ are given by equation (9), i.e.

$$\bar{T}_a = \begin{bmatrix} 0 & 0 \\ 0 & L^T Q_a L \end{bmatrix}; \quad \bar{R} = R + B^T \bar{T}_a B \tag{58}$$

and the derivative matrix Λ is given by

$$\Lambda = \frac{\partial \bar{q}}{\partial Z} = I + A^{-1} \frac{\partial \tilde{f}(Z)}{\partial Z} \tag{59}$$

For most civil engineering structures, the non-linear part $\tilde{f}(Z)$ of $\bar{q}(Z)$ and its derivative $\partial \tilde{f}(Z)/\partial Z$ are zero around the equilibrium point $Z = 0$. Consequently, $\Lambda_0 = \Lambda|_{Z=0} = I$. Matrices $\hat{P}$ and $\hat{M}_i$ in the controller, equation (57), are determined from steady-state Riccati and Lyapunov matrix equations,

$$\hat{P}\bar{A} + \bar{A}^T \hat{P} - \hat{P} B \bar{R}^{-1} B^T \hat{P} + \bar{Q} = 0 \tag{60}$$

$$\hat{M}_i(\bar{A} - B\bar{R}^{-1}B^T P) + (\bar{A} - B\bar{R}^{-1}B^T P)^T \hat{M}_i + Q_i = 0, \quad i = 2, 3, \ldots, k \tag{61}$$

where

$$\bar{A} = [A - B\bar{R}^{-1}B^T \bar{T}_a]; \quad \bar{Q} = Q + A^T \bar{T}_a A - A^T \bar{T}_a B \bar{R}^{-1} B^T \bar{T}_a A \tag{62}$$

Moreover, if matrices M_i's in equation (57) are determined from the solution of steady-state matrix Riccati equations instead of Lyapunov equations, i.e.

$$\hat{M}_i(\bar{A} - B\bar{R}^{-1}B^T \hat{P}) + (\bar{A} - B\bar{R}^{-1}B^T \hat{P})^T \hat{M}_i - \hat{M}_i B \bar{R}^{-1} B^T \hat{M}_i + Q_i = 0 \tag{63}$$

then the performance index to be minimized is given by equation (55) with

$$\bar{h}(\bar{q}) = \bar{h}_2(\bar{q}) = \bar{h}_1(\bar{q}) - \sum_{i=2}^{k} (\bar{q}^T M_i \bar{q})^{i-1} (\bar{q}^T M_i \Lambda B \bar{R}^{-1} B^T \Lambda^T M_i \bar{q}) \tag{64}$$

For linear structures in which $\tilde{f}(Z) = 0$, the optimal polynomial controller in equation (57) becomes

$$U(t) = -\bar{R}^{-1}B^T(\bar{T}_a + P)Z - \bar{R}^{-1}B^T \sum_{i=2}^{k} (Z^T M_i Z)^{i-1} M_i Z \tag{65}$$

When the penalty for acceleration response is removed from the performance index in Equation (55), i.e. $Q_a = 0$, it follows from equation (58) that $\bar{T}_a = 0$. The controller in equation (65) with $\bar{T}_a = 0$ is the same as the optimal polynomial controller presented in Agrawal and Yang[23,24] for linear structures.

REFERENCES

1. A. M. Reinhorn, T. T. Soong and C. Y. Yen, 'Base-isolated structures with active control', *Recent Advances in Design, Analysis, Testing and Qualification Methods*, PVP-Vol. 127, ASME, 1987, pp. 413–419.
2. B. F. Spencer Jr., J. Suhardjo and M. K. Sain, 'Nonlinear optimal control of a duffing system', *Int j nonlinear mech.* **27**, 157–172 (1992).
3. S. M. Nagarajaiah, M. A. Riley and A. M. Reinhorn, 'Hybrid control of sliding isolated bridges', *J. eng. mech. ASCE* **119**, 2317–2332 (1993).
4. A. M. Reinhorn, R. Subramaniam, S. M. Nagarajaiah and M. A. Riley, 'Study of hybrid systems for structural and nonstructural systems', in: G. W. Housner and S. F. Masri (eds), *Proc. int. workshop on structural control and intelligent system*, Honolulu, Hawaii, 1993, pp. 405–416.
5. M. A. Riley, R. Subramaniam, S. M. Nagarajaiah and A. M. Reinhorn, 'Hybrid control for sliding base-isolated structures', *Proc. ATC-17-1* seminar on seismic isolation, passive energy dissipation and active control, San Francisco, CA, 1993, pp. 799–810.
6. J. N. Yang, Z. Li and S. C. Liu, 'Stable controllers for instantaneous optimal control', *J. eng. mech. ASCE* **118**, 1612–1630 (1992).
7. J. N. Yang, Z. Li, J. C. Wu and I. R. Hsu, 'Dynamic linearization for sliding isolated building', *J. eng. struct.* **16**, 437–444 (1994).
8. J. N. Yang, Z. Li and S. Vongchavalitkul, 'A generalization of optimal control theory: linear and nonlinear control', *Tech. Report NCEER-92-0026*, National Center For Earthquake Engineering Research, Buffalo, 1992.
9. J. N. Yang, Z. Li and S. Vongchavalitkul, 'A generalization of optimal control theory: linear and nonlinear control', *J. eng. mech. ASCE* **120**, 266–283 (1994).

10. M. Dixon, B. Kermiche, P. B. Shing, R. Su and D. M. Frangopol, 'Design of hybrid control systems for building structures', *Proc. 10th eng. mech. specialty conf.*, Vol. 2, ASCE, Boulder, Colorado, 1995, pp. 1235–1238.
11. R. Krishnan, A. C. Nerves and M. P. Singh, 'Modeling, simulation and analysis of active control of structures with nonlinearity using neural networks', *Proc. 10th eng. mech. specialty conf.*, Vol. 2, ASCE, Boulder, Colorado, 1995, pp. 1054–1057.
12. J. N. Yang, J. C. Wu, A. K. Agrawal and Z. Li, 'Sliding mode control of seismic-excited linear and nonlinear civil engineering structures', *Tech. Report NCEER-94-0017*, National Center for Earthquake Engineering Research, Buffalo, 1994.
13. J. N. Yang, J. C. Wu and A. K. Agrawal, 'Sliding mode control of nonlinear and hysteretic structures', *J. eng. mech. ASCE*, **212**, 1330–1339 (1995).
14. J. N. Yang, J. C. Wu and A. K. Agrawal, 'Sliding mode control of seismic-excited linear structures', *J. eng. mech. ASCE* **212**, 1386–1390 (1995).
15. J. N. Yang, Z. Li and J. C. Wu 'Control of seismic-excited buildings using active variable stiffness systems', *Proc. 1994 Am. control conf.*, Baltimore, MD, 29 June–1 July, 1994, pp. 1083–1088.
16. J. N. Yang, J. C. Wu, K. Kawashima and S. Unjoh, 'Hybrid control systems for seismic-excited bridges', *J. earthquake eng. struct. dyn.* **24**, 1437–1451 (1995).
17. J. N. Yang, J. C. Wu, A. M. Reinhorn, M. Riley, W. E. Schmitendorf and F. Jabbari, 'Experimental verifications of H_∞ and sliding mode control for seismic-excited buildings', *J. struct. eng. ASCE* **122**, 69–75 (1996).
18. J. N. Yang, J. C. Wu, A. M. Reinhorn, M. Riley, 'Control of sliding-isolated buildings using sliding mode control', *J struct. eng. ASCE* **122**, 83–91, (1996).
19. J. N. Yang, Z. Li and J. C. Wu, 'Control of seismic-excited buildings using active variable stiffness systems', *J. eng. struct.*, **18**, 589–596 (1996).
20. G. W. Housner, T. T. Soong and S. F. Masri, 'Second generation of active structural control in civil engineering', *Proc. 1st world conf. on structural control*, Pasadena, CA, August 1994, panel 1–18.
21. Z. Wu, V. Gattulli, R. C. Lin and T. T. Soong, 'Implementable control laws for peak response reduction', *Proc. 1st world conf. on structural control*, Pasadena, CA, August 1994, pp. TP2-50–TP2-59.
22. D. P. Tomasula, B. F. Spencer Jr. and M. K. Sain, 'Limiting extreme structural responses using an efficient non-linear control law', *Proc. 1st world conf. on structural control*, Pasadena, CA, August 1994, pp. FP4-22–FP4-31.
23. A. K. Agrawal and J. N. Yang, 'Nonlinear optimal control of seismic-excited linear structures', *Proc. 10th eng. mech. specialty conf.*, Vol. 2, ASCE, Boulder, Colorado, 1995, pp. 1223–1226.
24. A. K. Agrawal and J. N. Yang, 'Optimal polynomial control of seismic-excited linear structures', *J. eng. mech. ASCE*, **122** (1996).
25. D. S. Bernstein, 'Nonquadratic cost and nonlinear feedback control', *Int. j. robust nonlinear control* **3**, 211–229 (1993).
26. B. D. O. Anderson and J. Moore, *Optimal Control: Linear Quadratic Methods*, Prentice-Hall International Editions, 1990.
27. M. Vidyasagar, *Nonlinear Systems Analysis*, 3rd edn, Prentice-Hall, Englewood Cliffs, NJ, 1993.
28. A. K. Agrawal and J. N. Yang, 'Hybrid control of seismic response using nonlinear output feedback', *Analysis and Computation, Proc. ASCE structures congress XIV*, Chicago, 1996, pp. 339–349.
29. A. K. Agrawal and J. N. Yang, 'Nonlinear optimal polynomial control for linear and nonlinear structures', *Tech. Report NCEER-95-0019*, National Center for Earthquake engineering research, Buffalo, 1995.